JCB Journal of Cell Biology

REPORT

Cdk1 phosphorylation of the dynein adapter Nde1 controls cargo binding from G2 to anaphase

Caitlin L. Wynne and Richard B. Vallee

Cytoplasmic dynein is involved in diverse cell cycle–dependent functions regulated by several accessory factors, including Nde1 and Ndel1. Little is known about the role of these proteins in dynein cargo binding, and less is known about their cell cycle–dependent dynein regulation. Using Nde1 RNAi, mutant cDNAs, and a phosphorylation site–specific antibody, we found a specific association of phospho-Nde1 with the late G2-M nuclear envelope and prophase to anaphase kinetochores, comparable to the pattern for the Nde1 interactor CENP-F. Phosphomutant-Nde1 associated only with prometaphase kinetochores and showed weaker CENP-F binding in in vitro assays. Nde1 RNAi caused severe delays in mitotic progression, which were substantially rescued by both phosphomimetic and phosphomutant Nde1. Expression of a dynein-binding–deficient Nde1 mutant reduced kinetochore dynein by half, indicating a major role for Nde1 in kinetochore dynein recruitment. These results establish CENP-F as the first well-characterized Nde1 cargo protein, and reveal phosphorylation control of Nde1 cargo binding throughout a substantial fraction of the cell cycle.

Introduction

Cytoplasmic dynein is a minus end–directed microtubule (MT) motor protein involved in a broad range of cellular functions throughout the cell cycle. However, mechanisms for cell cycle–dependent targeting of dynein to subcellular cargo remain incompletely understood. The dynein accessory proteins Nde1 and Ndel1 have been implicated along with LIS1 in regulating dynein motor behavior (McKenney et al., 2010; Huang et al., 2012) and potentially subcellular cargo binding (Stehman et al., 2007; Lam et al., 2010). Nde1 and Ndel1 are also phosphorylated by Cdk1 (Yan et al., 2003; Alkuraya et al., 2011), suggesting a novel role for this protein kinase in cell cycle regulation of dynein behavior.

Dynein localizes to the nuclear envelope (NE; Salina et al., 2002; Splinter et al., 2010; Bolhy et al., 2011) and mitotic kinetochores (Pfarr et al., 1990; Steuer et al., 1990; Wordeman et al., 1991; King et al., 2000). NE recruitment is via "early" and "late" G2 mechanisms involving Cdk1 phosphorylation of the nucleoporin RanBP2, which recruits BicD2, dynein, and dynactin (Splinter et al., 2010; Hu et al., 2013; Baffet et al., 2015) and Cdk1-dependent export of CENP-F from the nucleoplasm to associate with the nuclear surface via the nucleoporin Nup133 (Bolhy et al., 2011; Hu et al., 2013). CENP-F, in turn, recruits Nde1 and Ndel1 to the NE and mitotic kinetochores (Liang et al., 2007; Vergnolle and Taylor, 2007; Bolhy et al., 2011). How the latter behaviors are controlled is unknown.

Nde1 and Ndel1 are closely related paralogs implicated in a variety of dynein-mediated processes, including brain development, with a noteworthy role for human NDE1 mutations in microcephaly (Feng and Walsh, 2004; Alkuraya et al., 2011; Doobin et al., 2016). The Nde1 and Ndel1 proteins (also known as, NudE and NudEL) show 54% amino acid sequence identity and 73% similarity. Each contains an elongated N-terminal coiled-coil domain, which includes dynein and LIS1-binding sites (Sasaki et al., 2000; Derewenda et al., 2007; Wang and Zheng, 2011; Zyłkiewicz et al., 2011; Fig. 1 A). In vitro studies found Nde1 to recruits LIS1 and dynein into a supercomplex, which enhances the dynein–MT interaction under load, resulting in increased dynein force production in vitro (McKenney et al., 2010) and in vivo (Reddy et al., 2016). How Nde1 and Ndel1 serve in dynein cargo recruitment and how this behavior is regulated remain uncertain. Nde1 and Ndel1 interact through their C-terminal disordered regions (Fig. 1 A) with diverse proteins, including CENP-F, LC8, 14-3-3ε, DISC1, Su48, MCRS1/p78, and Ankyrin-G (Ozeki et al., 2003; Toyo-oka et al., 2003; Hirohashi et al., 2006a,b; Stehman et al., 2007; Vergnolle and Taylor, 2007; Kuijpers et al., 2016), some of which may serve in linking dynein to its cargo. Knockdown of CENP-F in particular decreases Nde1 and Ndel1's association with the G2 NE and mitotic kinetochores (Liang et al., 2007; Vergnolle and Taylor, 2007; Bolhy et al., 2011) and represents one of the

Pathology and Cell Biology, Columbia University, New York, NY.

Correspondence to Richard B. Vallee: rv2025@columbia.edu.

https://doi.org/10.1083/jcb.201707081

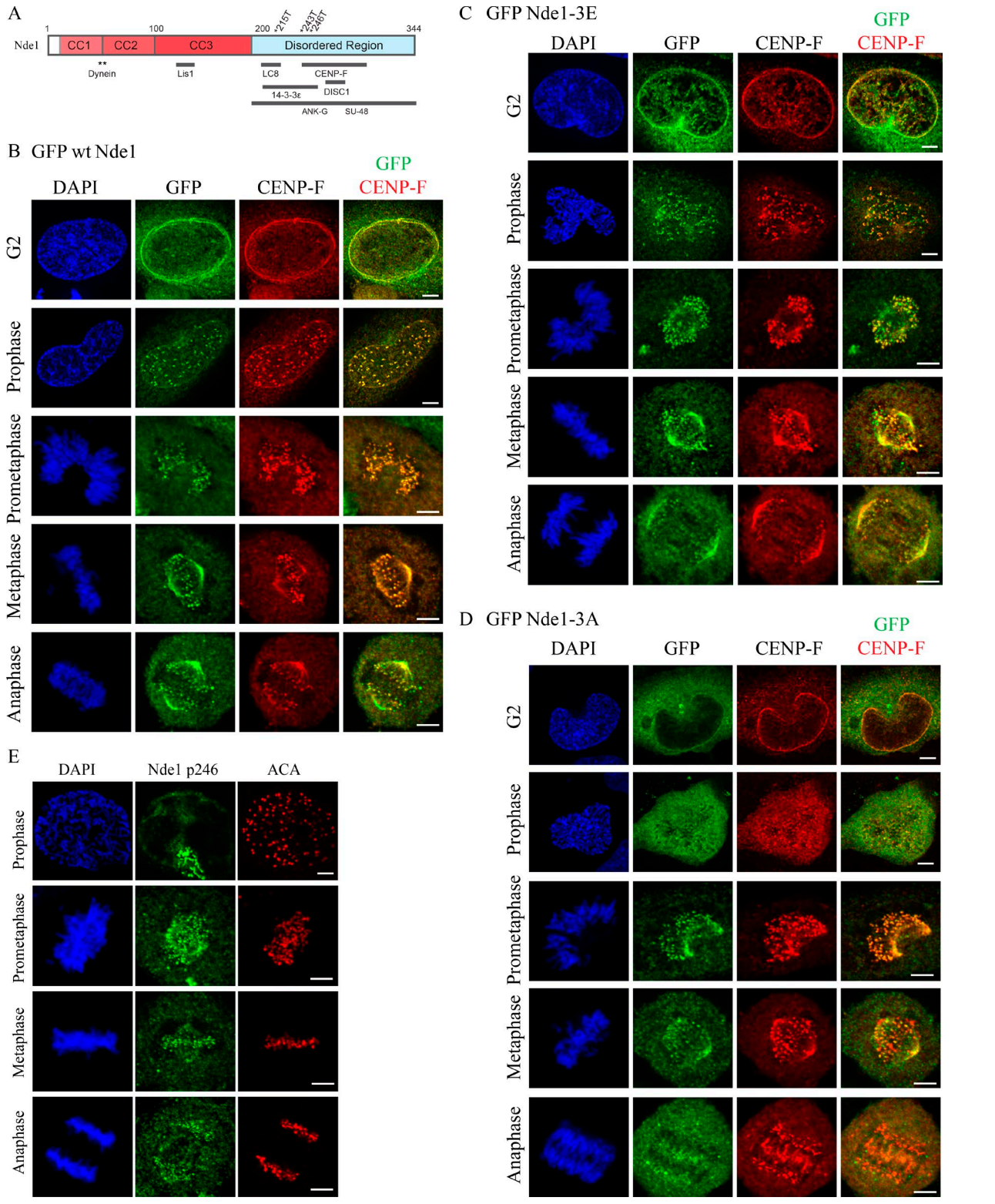

Figure 1. **Subcellular localization of Cdk1 phosphomimetic and phosphomutant Nde1 in G2 and mitosis. (A)** Diagram of Nde1 showing Cdk1 phosphorylation sites (T215, T243, and T246) and interaction sites. **(B–D)** HeLa cells were transfected with GFP-tagged WT, phosphomimetic, and phosphomutant Nde1 and examined for localization to the G2 NE and mitotic kinetochores. GFP was detected by immunocytochemistry. WT and phospho-Nde1 colocalize with CENP-F at the NE and prophase–anaphase kinetochores. The phosphomutant Nde1 was weakly detected at these sites and absent from metaphase and anaphase kinetochores. **(E)** HeLa cells were stained with CDK1-phospho-specific antibody (p246; Alkuraya et al., 2011), which reacted with prometaphase-to-anaphase kinetochores, consistent with the distribution of the expressed phosphomimetic Nde1. Bars, 5 µm.

more well-established candidates for an important role in Nde1/Ndel1–mediated dynein recruitment to cargo.

The specific mechanisms responsible for Nde1 and Ndel1 regulation are unknown, but these proteins contain phosphorylation sites for Cdk1, Cdk5, Aurora A, and Erk1/2 kinases (Stukenberg et al., 1997; Yan et al., 2003; Mori et al., 2007; Alkuraya et al., 2011). Expression of Cdk5 phosphomutant Ndel1 was found to affect lysosome motility in axons (Pandey and Smith, 2011; Klinman and Holzbaur, 2015) and to affect dynein and LIS1 binding in vitro (Hebbar et al., 2008; Zyłkiewicz et al., 2011). However, because phosphorylation sites are concentrated within the Nde1 and Ndel1 C-terminal regions, we suspected a role for phosphorylation in cargo binding. Cdk1 inhibition of an in vitro interaction between Nde1 and the centrosome protein Su48 has been reported (Hirohashi et al., 2006b), but a role for Cdk1 in regulating binding to more extensively established cargoes has not been investigated.

We report that Cdk1 phosphorylation of Nde1 stimulates CENP-F binding and is required for Nde1 targeting to the NE and kinetochores in vivo. Of considerable interest, GFP-tagged phosphomimetic Nde1 and endogenous phospho-Nde1 persist at kinetochores well beyond the metaphase/anaphase transition and through much of anaphase, similar to the behavior of CENP-F. These results, together with physiological analysis of Cdk1-phosphorylated Nde1 behavior, provide the first strong evidence that Nde1 phosphorylation regulates cargo binding and support prominent Nde1 roles in kinetochore function and mitotic progression.

Results and discussion

Differential distribution of phosphorylated versus dephosphorylated Nde1

We focused on Nde1 in particular because of its predominant role compared with Ndel1 in mitotic progression in HeLa cells (Vergnolle and Taylor, 2007) and in mitotic entry in neuronal progenitors (Doobin et al., 2016). To determine how Cdk1 phosphorylation may regulate Nde1-mediated dynein recruitment to cargo in vivo, we monitored the G2/M distribution of GFP-tagged WT Nde1 and triple phosphomimetic and triple phosphomutant Nde1 constructs (Nde1-3E and Nde1-3A, respectively). Mutations were at amino acids T215, T243, and T246, which are predicted and in vivo–demonstrated Cdk1 sites (Hirohashi et al., 2006b; Alkuraya et al., 2011). We found GFP-tagged WT Nde1 (GFP WT Nde1) to be detectable at the HeLa G2 NE and at prophase kinetochores before NE breakdown (NEBD) through prometaphase and metaphase and into anaphase (Fig. 1 B). This pattern was reminiscent of that for endogenous CENP-F (Rattner et al., 1993; Liao et al., 1995). We, indeed, found GFP WT Nde1 to colocalize with endogenous CENP-F throughout all stages of mitosis, consistent with immunocytochemical analysis (Fig. S1 A; Stehman et al., 2007). To test the role of Nde1 phosphorylation in this behavior, we examined the distribution of GFP Nde1-3E expressed in HeLa cells. Its pattern was comparable to that for GFP WT Nde1 at the G2 NE and mitotic kinetochores from before completion of NEBD through mid-anaphase (Fig. 1 C). In contrast, triple phosphomutant Nde1 (GFP Nde1-3A) exhibited reduced NE staining. The construct did show clear kinetochore localization during prometaphase, but strikingly, it was lost from kinetochores upon chromosome alignment (Fig. 1 D).

As a further test, we performed immunocytochemistry using an antibody raised against an Nde1 peptide phosphorylated by Cdk1 at residue T246 (Alkuraya et al., 2011; Materials and methods) and again saw clear staining at kinetochores from prometaphase through anaphase (Fig. 1 E). To assess the effect of MTs on this behavior, we treated transfected cells with nocodazole for 1 h and determined mean kinetochore-associated intensity for each of the GFP-Nde1 expression constructs (Fig. 2 A). The GFP Nde1-3A mutant exhibited an ∼50% reduction in intensity relative to Nde1-3E and an ∼62% reduction relative to GFP WT Nde1 (Fig. 2 B). In contrast, the distribution and kinetochore intensity of CENP-F staining was independent of GFP-Nde1 phosphorylation state (Fig. 2 C). These results suggest that Nde1 phosphorylation serves to increase its affinity for CENP-F and support an upstream position for CENP in the hierarchy of kinetochore interactors. To test the effects of Cdk1 phosphorylation on Nde1 kinetochore localization at metaphase, we treated cells with the proteasome inhibitor Mg132 (Fig. 2 D). Kinetochore-associated GFP Nde1-3A levels were substantially decreased relative to those of GFP WT Nde1 or Nde1-3E (Fig. 2 E). These results are consistent with specific dynein-mediated removal of the dephosphorylated Nde1 from attached kinetochores.

Effect of Nde1 phosphorylation on its interaction with CENP-F in vitro

The similar distribution pattern for phospho-Nde1 and CENP-F during mitotic progression suggested that Nde1 phosphorylation might affect its interaction with CENP-F. Because of the large size of CENP-F, we used a bacterially expressed GST-tagged fragment containing its Nde1-binding domain (NBD; Fig. 3 A; Vergnolle and Taylor, 2007). GST-CENP-F-NBD pulled down both Nde1-3E and Nde1-3A, but 2.5-fold higher levels of the former (Fig. 3 B). As an alternative approach, we used recombinant WT full-length Nde1 phosphorylated in vitro by incubation with recombinant Cdk1 + CyclinB. We again observed pull-down of 2.5-fold more phospho-Nde1 than dephospho-Nde1 (Fig. 3 C). Immunoprecipitation of the GFP-tagged Nde1 constructs also revealed significantly stronger coimmunoprecipitation of endogenous CENP-F by WT and phosphomimetic Nde1 (Fig. 3 D). Together, our results support the conclusion that Cdk1 phosphorylation of Nde1 enhances its NE and kinetochore binding through an increased affinity for CENP-F.

Role of Nde1 phosphorylation in mitotic progression

To determine the physiological role of Nde1 phosphorylation, we performed live-cell imaging of mitotic progression. Histone H2B-RFP–expressing HeLa cells were transfected with GFP or the GFP-Nde1 constructs and monitored from NEBD to anaphase onset (Fig. 4, A–D; and Fig. S2). Cells expressing GFP Nde1-3A took approximately twice as long to reach anaphase onset than cells expressing GFP, GFP WT Nde1, or GFP-Nde1-3E (Fig. 4 G). The delay for the phosphomutant Nde1 was typically associated with prolongation of late prometaphase and metaphase, consistent with a delay in MT attachment.

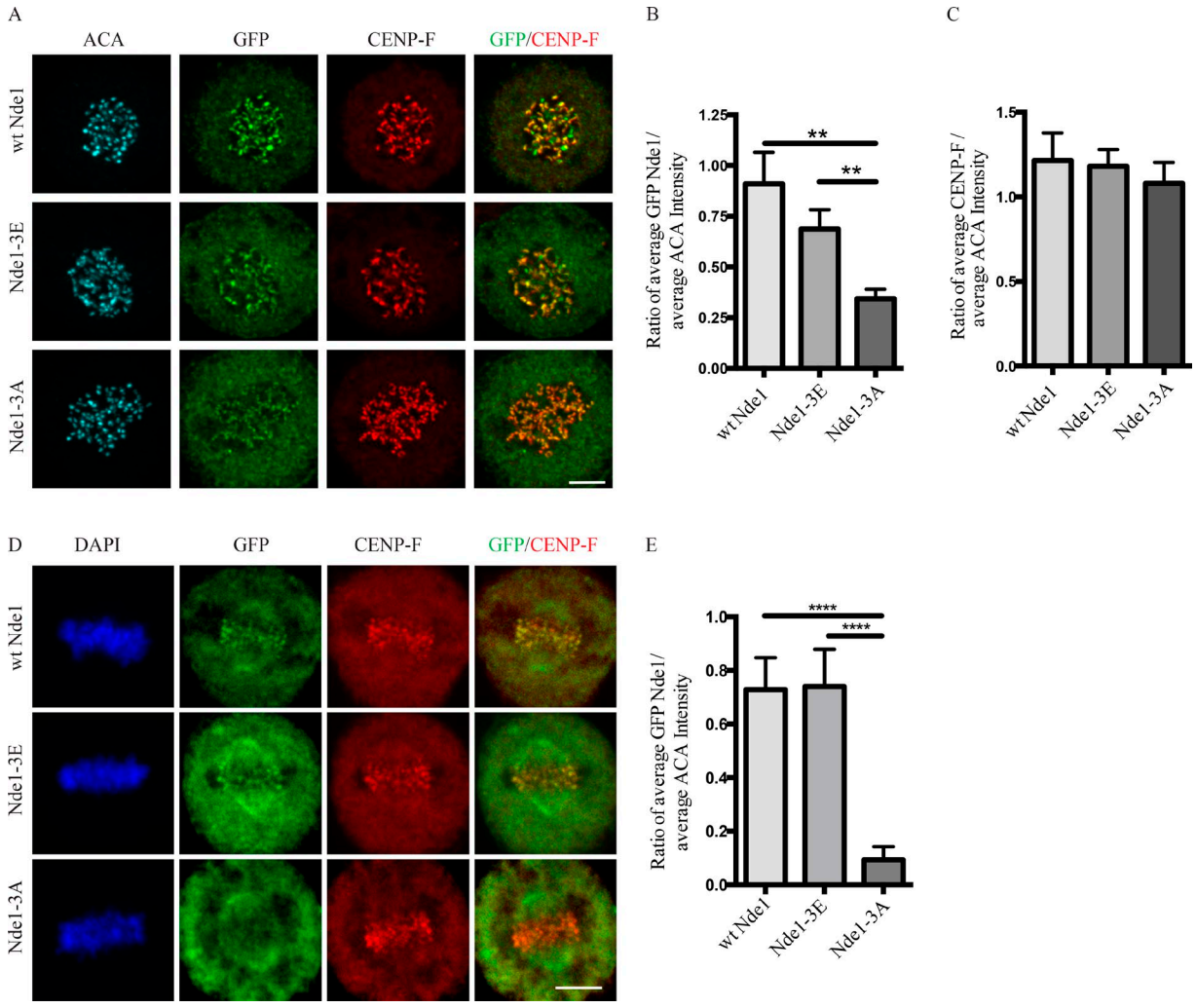

Figure 2. **Effects of Nde1 phosphorylation on localization at unattached kinetochores. (A)** Distribution of GFP-WT and phosphorylation-state mutant Nde1 in nocodazole-treated HeLa cells showing clear localization of each construct to kinetochores in the absence of MTs. The intensity of phosphomutant Nde1 appeared to be decreased relative to WT and phosphomimetic nde1. Bar, 5 µm. **(B)** Quantification of (anti-GFP vs. anti-ACA immunofluorescence intensity). Student's *t* test showed a significant decrease in phosphomutant Nde1 intensity relative to the other conditions. **, P < 0.005. **(C)** Quantification of mean CENP-F intensity relative to mean ACA immunofluorescence signal. ANOVA statistical analysis showed no significant difference among the three conditions. Mean ± SEM for three independent experiments is represented. **(D)** HeLa cells transfected Nde1 phosphorylation-state cDNAs were blocked at metaphase with the proteasome inhibitor MG132, and kinetochores were examined for GFP immunofluorescence intensity. The phosphomutant Nde1-3A was absent from the kinetochores, revealing that Cdk1 phosphorylation of Nde1 blocks its dynein-mediated removal from these sites. Bar, 5 µm. **(E)** Quantification of GFP Nde1 signal intensity at kinetochores relative to ACA immunofluorescence. Student's *t* test identified a significant decrease in levels of GFP Nde1-3A at kinetochores. ****, P < 0.0001.

To test further the effects of Cdk1 phosphorylation, we performed Nde1 RNAi and RNAi rescue. HeLa cells were transfected with Nde1 siRNAs, followed by RNAi-insensitive GFP-Nde1 cDNAs, and analyzed for delays in mitotic progression (Fig. 4, H–L; and Fig. S3). Nde1 RNAi caused a very substantial delay in reaching anaphase onset, as has been observed previously using this approach (Vergnolle and Taylor, 2007; Raaijmakers et al., 2013), microinjection of an Nde1/Ndel1 function–blocking antibody (Stehman et al., 2007), or expression of GFP-Nde1 dominant-negative fragments (Stehman et al., 2007). Surprisingly, rescue of Nde1 RNAi with WT Nde1, Nde1-3E, or Nde1-3A each reduced the mean time from NEBD to anaphase onset to a similar extent, though in no case completely to control levels (Fig. 4 O).

Nde1 recruitment of dynein and LIS1

To gain insight into the roles of discrete Nde1 interactions, we expressed Nde1 mutants defective in dynein or LIS1 binding (Nde1-del-dynein:Nde1-47A/51A and Nde1-del-Lis1:Nde1-118A/126A/129A, respectively; Derewenda et al., 2007; Zyłkiewicz et al., 2011; Fig. 4, E and F; and Fig. S2). Expression of GFP Nde1-del-dynein alone increased the time from NEBD to anaphase onset by approximately threefold in comparison to GFP alone or GFP WT Nde1. Cells typically exhibited substantial delays in chromosome alignment as well as metaphase duration. Cells expressing GFP Nde1-del-Lis1 demonstrated a smaller significant delay in mitotic progression (Fig. 4 G).

We also performed RNAi rescue analysis with RNAi-resistant forms of the deletion constructs (Figure 4, M and N; and Fig.

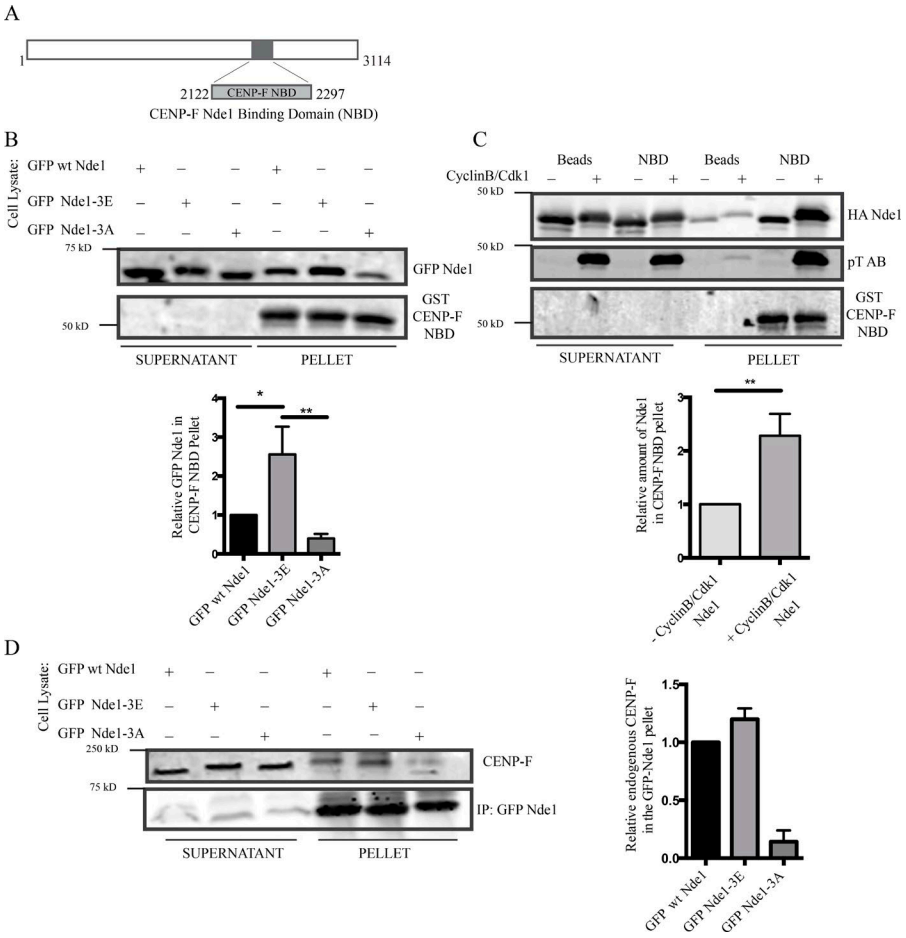

Figure 3. **Nde1 Cdk1 phosphorylation of Nde1 enhances CENP-F interaction. (A)** Diagram showing CENP-F fragment used for biochemical analysis (NBD: amino acids 2,122–2,297). **(B)** GST-CENP-F NBD pull-down of GPF-Nde1 constructs from HeLa cells demonstrates increased binding of GFP-phosphomimetic Nde1. **(C)** GST-CENP-F NBD pull-down of bacterially expressed HA-Nde1 after in vitro phosphorylation with recombinant Cdk1/CyclinB. Levels of Nde1 in the CENP-F NBD pull-downs were quantified and again revealed an increased binding of Cdk1-phosphorylated Nde1 to the GST CENP-F NBD fragment. **(D)** Anti-GFP immunoprecipitation of endogenous CENP-F with GFP-tagged Nde1 phosphorylation state constructs. Immunoprecipitation of GFP WT Nde1 and GFP-Nde1-3E each specially coprecipitated endogenous CENP-F. Mean ± SEM of three independent experiments is represented. **, $P < 0.005$; *, $P < 0.05$.

S3). We saw no rescue with the dynein-binding–deficient Nde1 construct, in contrast to the effects of the other Nde1 RNAi-resistant cDNAs. However, we found that RNAi-resistant Nde1-del-Lis1 reduced mitotic progression close to WT Nde1 levels (Fig. 4 O).

These experiments support a role for Nde1 in dynein recruitment to kinetochores (Stehman et al., 2007; Vergnolle and Taylor, 2007), in contrast to an earlier study (Raaijmakers et al., 2013). Using nocodazole-treated cells, we found Nde1 RNAi to decrease kinetochore dynein levels by ∼50%. WT Nde1 RNAi rescue largely restored kinetochore dynein, whereas little recovery was observed by rescue with Nde1-del-dynein (Fig. 5, A–C). We also rescued Nde1 knockdown with WT Nde1, Nde1-3E, or Nde1-3A and found dynein to be restored to similar levels independent of Nde1 phosphorylation state (Fig. 5, D and E). Thus, although Nde1 recruitment to the kinetochore is under Cdk1 control, Nde1 recruitment of dynein may be more or less constitutive. We reason that the selective disappearance of dynein from kinetochores must reflect self-removal of the motor protein, which also carries away checkpoint proteins, but not Nde1.

Role of Nde1 phosphorylation in vivo

Our data together identify a novel role for Nde1 phosphorylation in regulating its recruitment to the G2 NE and mitotic kinetochores. Phosphorylated Nde1 was observed to persist at kinetochores well beyond MT attachment and into anaphase. This behavior contrasts with that of dynein, dynactin (Pfarr et al., 1990; Steuer et al., 1990; Echeverri et al., 1996), and other dynein interactors (Faulkner et al., 2000; Griffis et al., 2007; Chan et al., 2009), which are depleted from kinetochores upon MT attachment. However, phospho-Nde1 behavior is clearly comparable to that of CENP-F, which also associates with the G2 NE and mitotic kinetochores, the latter well into anaphase (Rattner et al., 1993; Liao et al., 1995). Our finding that Cdk1 phosphorylation stimulates the physical interaction of Nde1 with CENP-F suggests a mechanism for controlling Nde1 distribution throughout late G2 to anaphase, the first evidence for phosphoregulation of Nde1 subcellular targeting. Given a reported role for Cdk5 phosphorylation in Ndel1-mediated axonal transport of lysosomes (Pandey and Smith, 2011; Klinman and Holzbaur, 2015), we speculate that phosphorylation might regulate the interaction of Nde1 and Ndel1 with vesicular factors as well.

How Cdk1-phosphorylated Nde1 can persist at anaphase kinetochores despite the well-established drop in Cdk1 activity at anaphase onset is unknown. An appealing possibility involves a potential role for proteins of the 14-3-3 family, which may protect Nde1's Cdk1 and Cdk5 sites from dephosphorylation (Toyooka et al., 2003).

In contrast to the phosphorylated form of Nde1, the GFP-tagged phosphomutant showed weak G2 NE decoration. It could be detected at prometaphase kinetochores, but at lower levels, and it was absent from metaphase and anaphase kinetochores

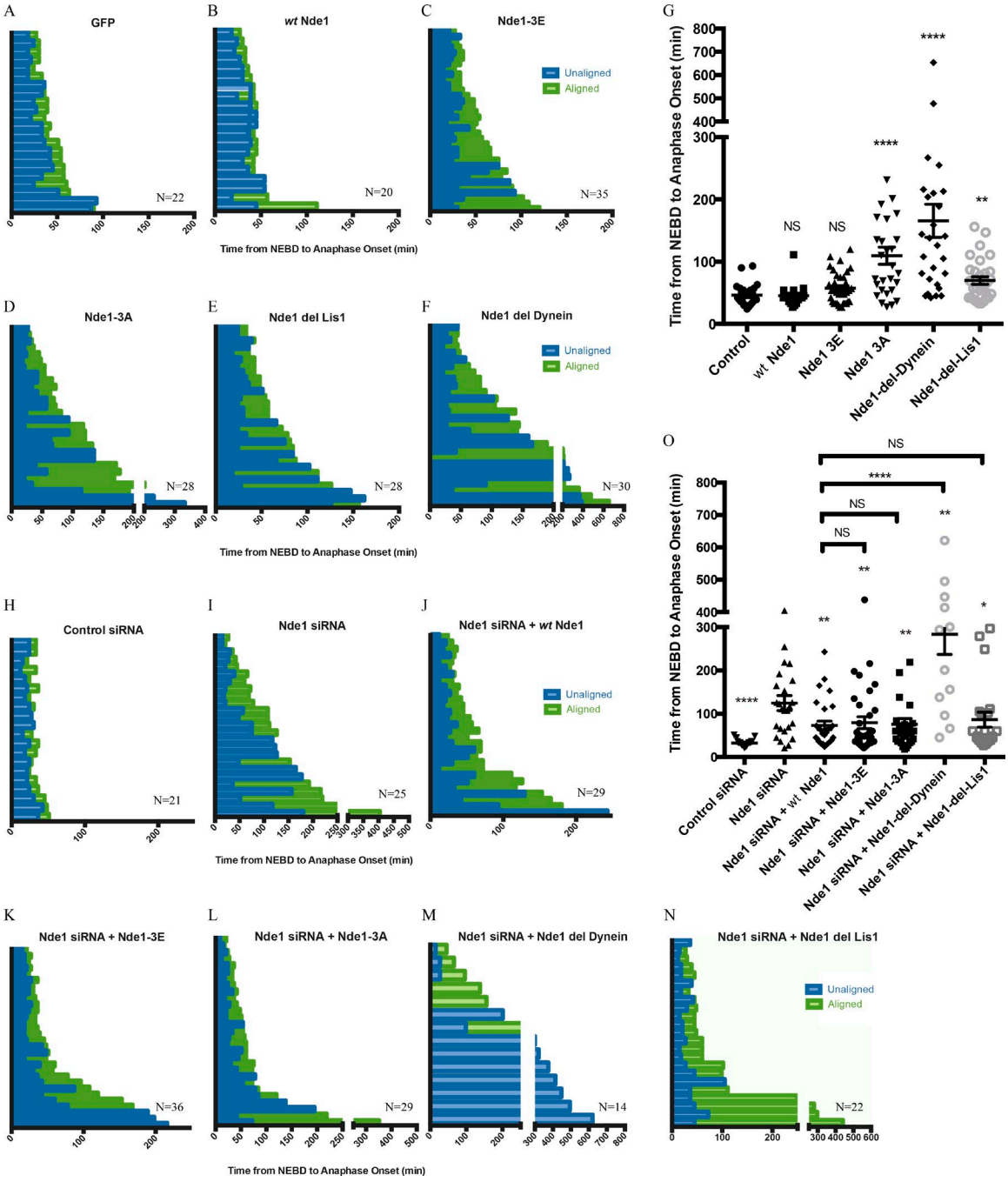

Figure 4. **Role of Nde1 phosphorylation in mitotic progression. (A–F)** Duration of mitotic events for individual H2B-RFP HeLa cells expressing GFP or GFP-tagged WT Nde1, Nde1-3E, Nde1-3A, Nde1-del-dynein, or Nde1-del-Lis1. **(G)** Duration of prometaphase ("unaligned") and metaphase ("aligned") is shown and replotted as the complete time from NEBD to anaphase onset. Mean ± SEM for each condition is shown. Mann–Whitney statistical tests revealed a significant increase in the time from NEBD to anaphase onset for cells expressing GFP Nde1-3A, GFP Nde1-del-dynein, and GFP Nde1-del-Lis1 relative to GFP alone control. **(H–N)** Same as above, but in H2B-RFP–expressing HeLa cells treated with control or Nde1 siRNAs for 48 h and then rescued with GFP, WT Nde1, Nde1-3E, Nde1-3A, Nde1-del-dynein, or Nde1-del-Lis1 for 24 h before live-cell imaging. **(O)** Data replotted as complete time from NEBD to anaphase onset. Mann–Whitney statistical tests were performed to compare Nde1 siRNA to each GFP Nde1 rescue condition. All of the Nde1 constructs to some extent rescued effects of Nde1RNAi, whereas Nde1-del-dynein showed no such effect. Mean ± SEM for each condition is shown. **, P < 0.01; *, P < 0.05; ****, P < 0.0001.

(Fig. 1 E). This pattern is consistent with a specific loss of dephospho-Nde1 from kinetochores upon end-on MT attachment, as observed for dynein itself and spindle assembly checkpoint proteins, though we have not observed clear evidence of streaming behavior with expressed or endogenous Nde1.

Phenotypic consequences of Nde1 phosphorylation

Nde1 knockdown caused a marked delay in anaphase onset, consistent with prior studies (Vergnolle and Taylor, 2007; Raaijmakers et al., 2013). On average, cells exhibited a prolonged period of chromosome alignment or remained longer in

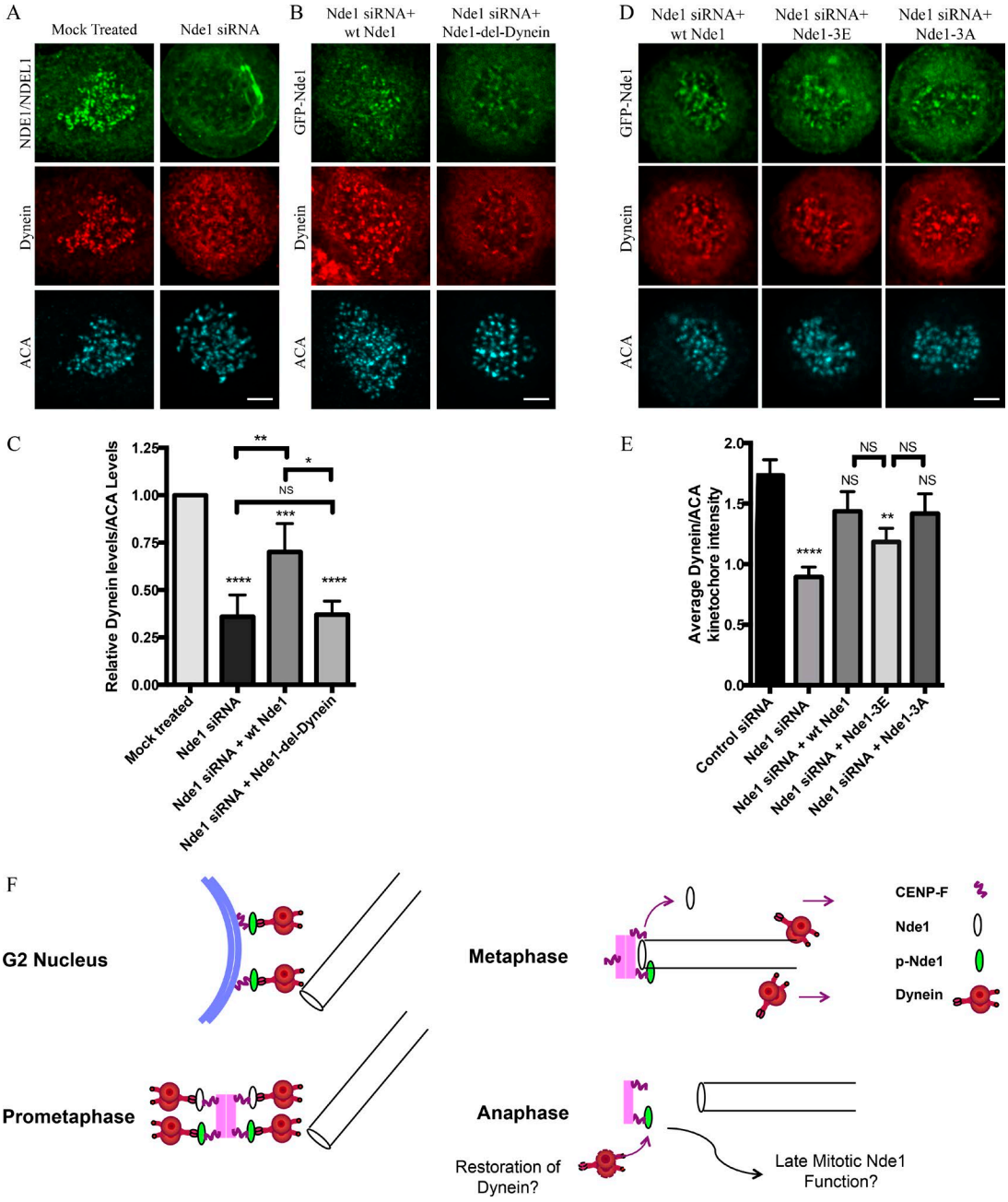

Figure 5. **Requirement of Nde1 for dynein recruitment to the kinetochore. (A)** HeLa cells treated with Nde1 siRNA, exposed to nocodazole, and immunostained for endogenous NDE1/NDEL1 or dynein intermediate chain. **(B)** Nde1 siRNA-treated HeLa cells rescued with expression of GFP WT Nde1 or GFP Nde1-del-dynein and stained for GFP and dynein intermediate chain. **(C)** Quantification of mean kinetochore dynein levels relative to mean ACA immunofluorescence signal. Dynein/ACA values were plotted ± SEM. Paired Student's *t* test was performed to analyze significance between conditions. **(D)** Nde1 siRNA-treated HeLa cells rescued by expression of WT Nde1, Nde1-3E, or Nde1-3A and stained for GFP and dynein intermediate chain. Bars, 5 µm. **(E)** Quantification of mean dynein intensity relative to mean ACA immunofluorescence signal. Mean ± SEM of three independent experiments is represented. Student's *t* tests were performed to analyze significance between conditions and revealed a significant difference in the levels of kinetochore dynein between Nde1 siRNA and WT Nde1, Nde1-3E, or Nde1-3A. *, $P < 0.05$; **, $P < 0.005$; ***, $P < 0.001$; ****, $P < 0.0001$. **(F)** Role of Cdk1 phosphorylation in G2-M Nde1 behavior. Phosphorylated Nde1 is shown associating with the G2 NE and then kinetochores from prophase into anaphase when dephosphorylated Nde1 is lost from these sites. Although dynein is undetectable at normal anaphase kinetochores, we speculate that persistent pNde1 might serve in a late dynein-mediated kinetochore attachment correction mechanism.

metaphase, consistent with our previous study reporting a role for Nde1 in dynein-dependent MT attachment and subsequent mitotic progression (Stehman et al., 2007). Most kinetochores were negative for Mad1/2 (unpublished data), suggesting that dynein-mediated checkpoint inactivation could still occur, but was incomplete because of a failure in proper MT attachment. Rescue with WT, phosphomimetic, or even phosphomutant Nde1 reduced the mitotic progression delays (Fig. 4 O). The latter case

seems surprising but may relate to the residual, albeit decreased, affinity of the phosphomutant Nde1 for prometaphase kinetochores (Fig. 3, B and C), Alternatively, our results may reflect an additional, as-yet-unidentified role for dephosphorylated Nde1. We note that, in addition to its contribution to kinetochore function, Nde1 has reported roles at the centrosome and spindle pole (Yan et al., 2003; Hirohashi et al., 2006b). Nde1 RNAi also disrupted spindle organization in some cells (unpublished data), which resisted RNAi rescue.

The reduction in kinetochore dynein levels by expression of Nde1-del-dynein is also striking and supports a prominent role for the Nde1–dynein interaction at these structures. Additional dynein interactors, including Zw10 of the RZZ complex, and spindly, have also been reported to contribute to kinetochore dynein recruitment (Starr et al., 1998; Griffis et al., 2007; Gassmann et al., 2008; Chan et al., 2009; Barisic et al., 2010; Cheerambathur et al., 2013; Gama et al., 2017). Multiple or dual recruitment pathways for dynein at the kinetochore as indicated here suggest functionally distinct kinetochore dynein pools, an important issue for future investigation. Additionally, our data (Fig. 5, D and E) are the first to highlight the unique role of Nde1 phosphorylation in directing the site and timing of its own kinetochore targeting and, through it, that of dynein.

Role for Nde1 phosphorylation in prolonged kinetochore association

Our results provide evidence that Cdk1 phosphorylation of Nde1 accounts for the unusual extended codistribution of Nde1 with CENP-F into anaphase, the physiological purpose of which, however, is uncertain. The *Caenorhabditis elegans* CENP-F homologue HCP1/2 has been reported to play a role in initiation of central spindle assembly (Maton et al., 2015). Nde1 and CENP-F might participate together in this or other, as-yet-unidentified late mitotic functions, a possibility requiring further investigation.

We speculate, alternatively, that CENP-F and Nde1 might persist at anaphase kinetochores as part of a rescue, or correction, mechanism. In this view, late defects in kinetochore–MT attachment might be rescued by renewed recruitment of dynein to kinetochores and chromosome recapture. We have in fact found that cells blocked in metaphase and then subjected to acute dynein inhibition lose proper kinetochore–MT attachment (Varma et al., 2008). Other results have supported a dynein contribution to anaphase A chromosome-to-pole movement (Savoian et al., 2000; Howell et al., 2001). Each of these observations supports potential residual activity for kinetochore dynein at this stage of mitosis, a role in which phosphorylated Nde1 might conceivably participate.

Materials and methods

Plasmids and molecular cloning

Mammalian expression constructs used in this study were pEGFP-C1 (Clonetech Laboratories) and derivatives of GFP mouse full-length WT Nde1 (Stehman et al., 2007). GFP-Nde1 3E (T215E, T242E, and T246E), GFP Nde1 3A (T215A, T242A, and T246A), GFP Nde1 del Lis1 (118A, 126A, and 129A), and GFP del dynein (47.51AA) were created by point mutagenesis of full-length GFP full-length WT Nde1 using site-directed point mutagenesis (Quickchange II; Agilent Technologies) with detailed primer sequences and their corresponding reverse complements. Primers for each mutant construct are as follows: Nde1 del dynein (5′-GCCGAGAATACGCAG CTGAATTGGCGGCTCAGCTGC-3′); Nde1 3E (primer 242E,246E: 5′-CCACTAGTGGGGAGCCACTCGAACCTGCAGCCCGG-3′ and 215E: 5′-GGCTCTGTACCGTCTGAGCCAGTAGCTCACCG-3′), Nde1 3A (primer 242A,246A: 5′-GCTCCACTAGTGGGGCGCCACTCGCAC CTGCAGCCCGG-3′ and 215A: 5′-GGCTCTGTACCGTCTGCTCCAGTA GCTCACCGAGG-3′), and Nde1 del Lis1 (primer 126A,129A: 5′-CCA ATGATGACCTGGAAGCAGCCAAAGCAGCCACAATCATGTCCC-3′ and 118A: 5′-GAAATACATTAGGGAACTGGCACAAGCCAATGATGA CCTGGAAAGAGCC-3′). Constructs containing three point mutations (Nde1 3E, Nde1 3A, and Nde1 del Lis1) were generated by sequential rounds of mutagenesis. All constructs were sequenced.

Cell culture reagents

HeLaM (a gift from V. Allen, University of Manchester, Manchester, England, UK) and HeLa H2B-RFP (a gift from R. King, Harvard Medical School, Boston, MA) were cultured in DMEM supplemented with 10% heat inactivated FBS and penicillin streptomycin. Transient transfections were performed using Effectene transfection reagent (Qiagen) according to the manufacturer's protocol. Protein knockdown was achieved using Dharmacon smartpool siRNAs (human Nde1 smartpool siRNA M-020625-00-0010 or control siRNA D-001810-01-05). HeLaM or HeLa H2B-RFP culture cells were transfected with 2 µM siRNA using Hiperfect reagent (Qiagen) for 48 h followed by fixation or live-cell imaging. Rescue experiments were performed using mouse Nde1 cDNA insensitive to human siRNA constructs. Rescue constructs GFP WT Nde1 and GFP Nde1 mutants were transfected in siRNA-treated cells 24 h before fixation or live-cell imaging. For drug treatments, HeLaM cells were treated with nocodazole for 1 h at 2.5 µM or with MG132 (Sigma) for 1 h at 10 µM before fixation.

Immunocytochemistry and Immunofluorescent microscopy

Cells were fixed in cold methanol for 7–10 min at −20° or with 3–4% PFAs in PBS buffer for 20 min at RT. PFA-fixed cells were subjected to preextraction with 0.05% Triton X-100 in PBS for 15 s and washed before fixation. PFA-fixed cells were permeabilized for 2 min with 0.5% Triton X-100 in PBS. Coverslips were blocked with 5% Normal Donkey Serum in PBS for 1 h at RT. Primary antibodies were added for 1 h at 37°C or overnight at 4°C and then washed before application of secondary antibodies (Cy2, Cy3, or Cy5; Jackson Labs) for 1 h at RT. Secondary antibodies were used at 1:300. DAPI was added to the second wash after secondary antibody. Coverslips stained for phospho-Nde1 with rabbit p246 were fixed with cold methanol at −20° followed by blocking with 5% Normal Donkey Serum and 0.05% Triton X-100 in TBS (20 mM Tris and 150 mM NaCl). Images were acquired with an IX83 Andor Revolution XD Spinning Disk Confocal System with a 60× silicone oil objective (NA 1.30) and a 2× magnifier coupled to an iXon Ultra 888 EMCCD Camera. Z-stacks of 0.5 µm were taken for each image.

Antibodies

Antibodies used in this study included rabbit polyclonal NudE/NudEL antibody (as generated in Stehman et al., 2007), human

Mitosin (CENP-Fl BD Biosciences), human CREST autoimmune serum anti (Antibodies, Inc.), mouse GST (Santa Cruz), mouse HA (Covance), rabbit GFP (Invitrogen), mouse tubulin (Abcam), mouse dynein intermediate chain (74.1; a gift from K. Pfister, University of Virginia, Charlottesville, VA), mouse phosphothreonine MAPK/CDK1 substrate AB (Cell Signaling), and rabbit p246 phospho-NudE antibody (a gift from Y. Feng, Northwestern University Feinberg School of Medicine, Chicago, IL; Alkuraya et al., 2011).

Live imaging

H2B-RFP HeLa cells were plated on 50-mm glass-bottom dishes (Mattek) and imaged in CO_2-independent media (Gibco) supplemented with 1 mM Glutamate and 10% FBS. Live-cell movies were taken with IX83 Andor Revolution XD Spinning Disk Confocal System with a 20× air objective (NA 0.7). Images were taken at a 3-min interval for a time course of 12–16 h.

Data quantification and statistics

Imaging data were analyzed with ImageJ software. Quantification of relative kinetochore intensity was calculated using the mean maximum fluorescence of a kinetochore relative to the mean maximum anti-centromere antibody (ACA) intensity: (mean maximum intensity – mean background intensity)/(mean maximum ACA intensity – mean ACA background intensity). Between 25 and 50 kinetochore measurements were taken per cell, and 15–20 measurements of the background intensity were polled to give the mean background intensity. At least 15 cells from three independent experiments were analyzed. Statistical analysis was performed using Excel (Microsoft) or Prism (GraphPad) software. Significance was determined by ANOVA, Student's *t* test, or Mann–Whitney test (*, $P < 0.05$; **, $P < 0.01$; ***, $P < 0.001$). Data represent mean ± SEM of at least three independent replicates.

Protein purification

Human CENP-F fragment (CENP-F NBD) was synthesized (Blue Heron) and cloned into pGex 6p-1 using BamHI and XhoI. pGex mouse Nde1 was previously described (Stehman et al., 2007; McKenney et al., 2010). GST Nde1 and GST CENP-F NBD constructs were purified by glutathione-sepharose affinity chromatography. Purified GST-tagged protein was either cleaved off glutathione beads (USB) by precision protease (GE Biosciences) or eluted with 10 mM of reduced glutathione. Buffer exchange with NAP-10 columns (GE Life Sciences) was performed to have the final purified protein in storage buffer (1 mM EDTA, 150 mM NaCl, 50 mM Tris, pH 7.0, 10% glycerol, and 1 mM DTT) or DB buffer (35 mM Pipes, 5 mM $MgSO_4$, 1 mM EGTA, 0.5 mM EDTA, and 1 mM DTT). Aliquots of purified protein were flash frozen in liquid nitrogen and stored at −80°.

In vitro kinase assay

CyclinB/Cdk1 protein kinase (Millipore) was used to perform in vitro Cdk1 kinase assays. 250 ng CyclinB/Cdk1 was incubated with 5–10 µg of bacterially purified recombinant mouse Nde1, 200 µM ATP, and 5× PK (NEB) buffer in a total volume of 50 µl. The reaction was incubated at 30° for 1 h. Phosphorylated Nde1 was then used in pull-down experiments. Phosphorylation of Nde1 was monitored by Western blot with phosphothreonine MAPK/CDK1 antibody.

Immunoprecipitation and pull-down experiments

Mammalian cell lysates were prepared in RIPA buffer, pH 7.4 (100 mM NaCl, 1 mM EGTA, 50 mM Tris, 1% NP-40, 1 mM DTT, and 1:100 protease inhibitor [Sigma]). Extracts were lysed on ice followed by centrifugation to remove the membranous fraction. 500–750 µg cell lysate was incubated with 5 µg antibody or added to GST-bound recombinant protein. Recombinant protein interaction studies were performed in buffer A (50 mM Hepes, pH 7.4, 150 mM NaCl, 1% NP-40, and 1 mM DTT). For CENP-F NBD GST pull-down experiments, eluted GST-NBD was incubated with glutathione agarose beads (USB) in buffer A for 1 h, washed, and then incubated with cell lysate expressing GFP Nde1 constructs or recombinant Nde1 for 1–3 h in a total volume of 300 µl. Beads were washed four times before addition of 50 µl RIPA or buffer A and 6× sample buffer. Samples were analyzed by SDS-PAGE gel and Western blot. Western blot analysis was performed with a methanol-activated polyvinylidene fluoride membrane (Millipore). The membrane was blocked with 5% milk in PBS for 1 h at RT. Primary antibodies were diluted in 5 ml of 5% milk in PBS, incubated with membrane for 1 h at RT or overnight at 4°, and then washed three times with PBS. Secondary antibodies (or 680 nm or 800 nm conjugated; LI-COR) were added to 5 ml of 5% milk in PBS at a dilution of 1:10,000 and incubated at RT for 1 h. The membrane was developed using the Odyssey Imaging system (LI-COR). Analysis of the membrane was performed using ImageJ software.

Online supplemental material

Fig. S1 shows the relative distribution of NDE1/NDEL1 and CENP-F during late G2 and mitosis. Fig. S2 shows the effect of in Nde1 mutants on chromosome behavior. Fig. S3 shows the effect of Ndel1 RNAi rescue on chromosome behavior.

Acknowledgments

We thank Dr. Yuanyi Feng for the phospho-specific Nde1 antibody; Dr. R. King for HeLa H2B-RFP cells; Drs. Y. Mao, T. Dantas, C. Bertipaglia, and J. Canman for extensive advice on the project and the manuscript; and C. Bertipaglia and J. Yi for extensive postsubmission contributions.

This work was supported by the National Institutes of Health (grants GM102347 and HD040182).

The authors declare no competing financial interests.

Author contributions: C.L. Wynne and R.B. Vallee conceived the project, carried out the experiments, and prepared the manuscript.

Submitted: 17 July 2017
Revised: 6 April 2018
Accepted: 23 May 2018

References

Alkuraya, F.S., X. Cai, C. Emery, G.H. Mochida, M.S. Al-Dosari, J.M. Felie, R.S. Hill, B.J. Barry, J.N. Partlow, G.G. Gascon, et al. 2011. Human mutations in NDE1 cause extreme microcephaly with lissencephaly [corrected]. *Am. J. Hum. Genet.* 88:536–547. https://doi.org/10.1016/j.ajhg.2011.04.003

Baffet, A.D., D.J. Hu, and R.B. Vallee. 2015. Cdk1 Activates Pre-mitotic Nuclear Envelope Dynein Recruitment and Apical Nuclear Migration in Neural Stem Cells. *Dev. Cell.* 33:703–716. https://doi.org/10.1016/j.devcel.2015.04.022

Barisic, M., B. Sohm, P. Mikolcevic, C. Wandke, V. Rauch, T. Ringer, M. Hess, G. Bonn, and S. Geley. 2010. Spindly/CCDC99 is required for efficient chromosome congression and mitotic checkpoint regulation. *Mol. Biol. Cell.* 21:1968–1981. https://doi.org/10.1091/mbc.e09-04-0356

Bolhy, S., I. Bouhlel, E. Dultz, T. Nayak, M. Zuccolo, X. Gatti, R. Vallee, J. Ellenberg, and V. Doye. 2011. A Nup133-dependent NPC-anchored network tethers centrosomes to the nuclear envelope in prophase. *J. Cell Biol.* 192:855–871. https://doi.org/10.1083/jcb.201007118

Chan, Y.W., L.L. Fava, A. Uldschmid, M.H. Schmitz, D.W. Gerlich, E.A. Nigg, and A. Santamaria. 2009. Mitotic control of kinetochore-associated dynein and spindle orientation by human Spindly. *J. Cell Biol.* 185:859–874. https://doi.org/10.1083/jcb.200812167

Cheerambathur, D.K., R. Gassmann, B. Cook, K. Oegema, and A. Desai. 2013. Crosstalk between microtubule attachment complexes ensures accurate chromosome segregation. *Science.* 342:1239–1242. https://doi.org/10.1126/science.1246232

Derewenda, U., C. Tarricone, W.C. Choi, D.R. Cooper, S. Lukasik, F. Perrina, A. Tripathy, M.H. Kim, D.S. Cafiso, A. Musacchio, and Z.S. Derewenda. 2007. The structure of the coiled-coil domain of Ndel1 and the basis of its interaction with Lis1, the causal protein of Miller-Dieker lissencephaly. *Structure.* 15:1467–1481. https://doi.org/10.1016/j.str.2007.09.015

Doobin, D.J., S. Kemal, T.J. Dantas, and R.B. Vallee. 2016. Severe NDE1-mediated microcephaly results from neural progenitor cell cycle arrests at multiple specific stages. *Nat. Commun.* 7:12551. https://doi.org/10.1038/ncomms12551

Echeverri, C.J., B.M. Paschal, K.T. Vaughan, and R.B. Vallee. 1996. Molecular characterization of the 50-kD subunit of dynactin reveals function for the complex in chromosome alignment and spindle organization during mitosis. *J. Cell Biol.* 132:617–633. https://doi.org/10.1083/jcb.132.4.617

Faulkner, N.E., D.L. Dujardin, C.Y. Tai, K.T. Vaughan, C.B. O'Connell, Y. Wang, and R.B. Vallee. 2000. A role for the lissencephaly gene LIS1 in mitosis and cytoplasmic dynein function. *Nat. Cell Biol.* 2:784–791. https://doi.org/10.1038/35041020

Feng, Y., and C.A. Walsh. 2004. Mitotic spindle regulation by Nde1 controls cerebral cortical size. *Neuron.* 44:279–293. https://doi.org/10.1016/j.neuron.2004.09.023

Gama, J.B., C. Pereira, P.A. Simões, R. Celestino, R.M. Reis, D.J. Barbosa, H.R. Pires, C. Carvalho, J. Amorim, A.X. Carvalho, et al. 2017. Molecular mechanism of dynein recruitment to kinetochores by the Rod-Zw10-Zwilch complex and Spindly. *J. Cell Biol.* 216:943–960. https://doi.org/10.1083/jcb.201610108

Gassmann, R., A. Essex, J.S. Hu, P.S. Maddox, F. Motegi, A. Sugimoto, S.M. O'Rourke, B. Bowerman, I. McLeod, J.R. Yates III, et al. 2008. A new mechanism controlling kinetochore-microtubule interactions revealed by comparison of two dynein-targeting components: SPDL-1 and the Rod/Zwilch/Zw10 complex. *Genes Dev.* 22:2385–2399. https://doi.org/10.1101/gad.1687508

Griffis, E.R., N. Stuurman, and R.D. Vale. 2007. Spindly, a novel protein essential for silencing the spindle assembly checkpoint, recruits dynein to the kinetochore. *J. Cell Biol.* 177:1005–1015. https://doi.org/10.1083/jcb.200702062

Hebbar, S., M.T. Mesngon, A.M. Guillotte, B. Desai, R. Ayala, and D.S. Smith. 2008. Lis1 and Ndel1 influence the timing of nuclear envelope breakdown in neural stem cells. *J. Cell Biol.* 182:1063–1071. https://doi.org/10.1083/jcb.200803071

Hirohashi, Y., Q. Wang, Q. Liu, X. Du, H. Zhang, N. Sato, and M.I. Greene. 2006a. p78/MCRS1 forms a complex with centrosomal protein Nde1 and is essential for cell viability. *Oncogene.* 25:4937–4946. https://doi.org/10.1038/sj.onc.1209500

Hirohashi, Y., Q. Wang, Q. Liu, B. Li, X. Du, H. Zhang, K. Furuuchi, K. Masuda, N. Sato, and M.I. Greene. 2006b. Centrosomal proteins Nde1 and Su48 form a complex regulated by phosphorylation. *Oncogene.* 25:6048–6055. https://doi.org/10.1038/sj.onc.1209637

Howell, B.J., B.F. McEwen, J.C. Canman, D.B. Hoffman, E.M. Farrar, C.L. Rieder, and E.D. Salmon. 2001. Cytoplasmic dynein/dynactin drives kinetochore protein transport to the spindle poles and has a role in mitotic spindle checkpoint inactivation. *J. Cell Biol.* 155:1159–1172. https://doi.org/10.1083/jcb.200105093

Hu, D.J., A.D. Baffet, T. Nayak, A. Akhmanova, V. Doye, and R.B. Vallee. 2013. Dynein recruitment to nuclear pores activates apical nuclear migration and mitotic entry in brain progenitor cells. *Cell.* 154:1300–1313. https://doi.org/10.1016/j.cell.2013.08.024

Huang, J., A.J. Roberts, A.E. Leschziner, and S.L. Reck-Peterson. 2012. Lis1 acts as a "clutch" between the ATPase and microtubule-binding domains of the dynein motor. *Cell.* 150:975–986. https://doi.org/10.1016/j.cell.2012.07.022

King, J.M., T.S. Hays, and R.B. Nicklas. 2000. Dynein is a transient kinetochore component whose binding is regulated by microtubule attachment, not tension. *J. Cell Biol.* 151:739–748. https://doi.org/10.1083/jcb.151.4.739

Klinman, E., and E.L. Holzbaur. 2015. Stress-Induced CDK5 Activation Disrupts Axonal Transport via Lis1/Ndel1/Dynein. *Cell Reports.* 12:462–473. https://doi.org/10.1016/j.celrep.2015.06.032

Kuijpers, M., D. van de Willige, A. Freal, A. Chazeau, M.A. Franker, J. Hofenk, R.J. Rodrigues, L.C. Kapitein, A. Akhmanova, D. Jaarsma, and C.C. Hoogenraad. 2016. Dynein Regulator NDEL1 Controls Polarized Cargo Transport at the Axon Initial Segment. *Neuron.* 89:461–471. https://doi.org/10.1016/j.neuron.2016.01.022

Lam, C., M.A. Vergnolle, L. Thorpe, P.G. Woodman, and V.J. Allan. 2010. Functional interplay between LIS1, NDE1 and NDEL1 in dynein-dependent organelle positioning. *J. Cell Sci.* 123:202–212. https://doi.org/10.1242/jcs.059337

Liang, Y., W. Yu, Y. Li, L. Yu, Q. Zhang, F. Wang, Z. Yang, J. Du, Q. Huang, X. Yao, and X. Zhu. 2007. Nudel modulates kinetochore association and function of cytoplasmic dynein in M phase. *Mol. Biol. Cell.* 18:2656–2666. https://doi.org/10.1091/mbc.e06-04-0345

Liao, H., R.J. Winkfein, G. Mack, J.B. Rattner, and T.J. Yen. 1995. CENP-F is a protein of the nuclear matrix that assembles onto kinetochores at late G2 and is rapidly degraded after mitosis. *J. Cell Biol.* 130:507–518. https://doi.org/10.1083/jcb.130.3.507

Maton, G., F. Edwards, B. Lacroix, M. Stefanutti, K. Laband, T. Lieury, T. Kim, J. Espeut, J.C. Canman, and J. Dumont. 2015. Kinetochore components are required for central spindle assembly. *Nat. Cell Biol.* 17:953. https://doi.org/10.1038/ncb3199

McKenney, R.J., M. Vershinin, A. Kunwar, R.B. Vallee, and S.P. Gross. 2010. LIS1 and NudE induce a persistent dynein force-producing state. *Cell.* 141:304–314. https://doi.org/10.1016/j.cell.2010.02.035

Mori, D., Y. Yano, K. Toyo-oka, N. Yoshida, M. Yamada, M. Muramatsu, D. Zhang, H. Saya, Y.Y. Toyoshima, K. Kinoshita, et al. 2007. NDEL1 phosphorylation by Aurora-A kinase is essential for centrosomal maturation, separation, and TACC3 recruitment. *Mol. Cell. Biol.* 27:352–367. https://doi.org/10.1128/MCB.00878-06

Ozeki, Y., T. Tomoda, J. Kleiderlein, A. Kamiya, L. Bord, K. Fujii, M. Okawa, N. Yamada, M.E. Hatten, S.H. Snyder, et al. 2003. Disrupted-in-Schizophrenia-1 (DISC-1): mutant truncation prevents binding to NudE-like (NUDEL) and inhibits neurite outgrowth. *Proc. Natl. Acad. Sci. USA.* 100:289–294. https://doi.org/10.1073/pnas.0136913100

Pandey, J.P., and D.S. Smith. 2011. A Cdk5-dependent switch regulates Lis1/Ndel1/dynein-driven organelle transport in adult axons. *J. Neurosci.* 31:17207–17219. https://doi.org/10.1523/JNEUROSCI.4108-11.2011

Pfarr, C.M., M. Coue, P.M. Grissom, T.S. Hays, M.E. Porter, and J.R. McIntosh. 1990. Cytoplasmic dynein is localized to kinetochores during mitosis. *Nature.* 345:263–265. https://doi.org/10.1038/345263a0

Raaijmakers, J.A., M.E. Tanenbaum, and R.H. Medema. 2013. Systematic dissection of dynein regulators in mitosis. *J. Cell Biol.* 201:201–215. https://doi.org/10.1083/jcb.201208098

Rattner, J.B., A. Rao, M.J. Fritzler, D.W. Valencia, and T.J. Yen. 1993. CENP-F is a. ca 400 kDa kinetochore protein that exhibits a cell-cycle dependent localization. *Cell Motil. Cytoskeleton.* 26:214–226. https://doi.org/10.1002/cm.970260305

Reddy, B.J., M. Mattson, C.L. Wynne, O. Vadpey, A. Durra, D. Chapman, R.B. Vallee, and S.P. Gross. 2016. Load-induced enhancement of Dynein force production by LIS1-NudE in vivo and in vitro. *Nat. Commun.* 7:12259. https://doi.org/10.1038/ncomms12259

Salina, D., K. Bodoor, D.M. Eckley, T.A. Schroer, J.B. Rattner, and B. Burke. 2002. Cytoplasmic dynein as a facilitator of nuclear envelope breakdown. *Cell.* 108:97–107. https://doi.org/10.1016/S0092-8674(01)00628-6

Sasaki, S., A. Shionoya, M. Ishida, M.J. Gambello, J. Yingling, A. Wynshaw-Boris, and S. Hirotsune. 2000. A LIS1/NUDEL/cytoplasmic dynein heavy chain complex in the developing and adult nervous system. *Neuron.* 28:681–696. https://doi.org/10.1016/S0896-6273(00)00146-X

Savoian, M.S., M.L. Goldberg, and C.L. Rieder. 2000. The rate of poleward chromosome motion is attenuated in Drosophila zw10 and rod mutants. *Nat. Cell Biol.* 2:948–952. https://doi.org/10.1038/35046605

Splinter, D., M.E. Tanenbaum, A. Lindqvist, D. Jaarsma, A. Flotho, K.L. Yu, I. Grigoriev, D. Engelsma, E.D. Haasdijk, N. Keijzer, et al. 2010. Bicaudal D2, dynein, and kinesin-1 associate with nuclear pore complexes and regulate centrosome and nuclear positioning during mitotic entry. *PLoS Biol.* 8:e1000350. https://doi.org/10.1371/journal.pbio.1000350

Starr, D.A., B.C. Williams, T.S. Hays, and M.L. Goldberg. 1998. ZW10 helps recruit dynactin and dynein to the kinetochore. *J. Cell Biol.* 142:763–774. https://doi.org/10.1083/jcb.142.3.763

Stehman, S.A., Y. Chen, R.J. McKenney, and R.B. Vallee. 2007. NudE and NudEL are required for mitotic progression and are involved in dynein recruitment to kinetochores. *J. Cell Biol.* 178:583–594. https://doi.org/10.1083/jcb.200610112

Steuer, E.R., L. Wordeman, T.A. Schroer, and M.P. Sheetz. 1990. Localization of cytoplasmic dynein to mitotic spindles and kinetochores. *Nature.* 345:266–268. https://doi.org/10.1038/345266a0

Stukenberg, P.T., K.D. Lustig, T.J. McGarry, R.W. King, J. Kuang, and M.W. Kirschner. 1997. Systematic identification of mitotic phosphoproteins. *Curr. Biol.* 7:338–348. https://doi.org/10.1016/S0960-9822(06)00157-6

Toyo-oka, K., A. Shionoya, M.J. Gambello, C. Cardoso, R. Leventer, H.L. Ward, R. Ayala, L.H. Tsai, W. Dobyns, D. Ledbetter, et al. 2003. 14-3-3epsilon is important for neuronal migration by binding to NUDEL: a molecular explanation for Miller-Dieker syndrome. *Nat. Genet.* 34:274–285. https://doi.org/10.1038/ng1169

Varma, D., P. Monzo, S.A. Stehman, and R.B. Vallee. 2008. Direct role of dynein motor in stable kinetochore-microtubule attachment, orientation, and alignment. *J. Cell Biol.* 182:1045–1054. https://doi.org/10.1083/jcb.200710106

Vergnolle, M.A., and S.S. Taylor. 2007. Cenp-F links kinetochores to Ndel1/Nde1/Lis1/dynein microtubule motor complexes. *Curr. Biol.* 17:1173–1179. https://doi.org/10.1016/j.cub.2007.05.077

Wang, S., and Y. Zheng. 2011. Identification of a novel dynein binding domain in nudel essential for spindle pole organization in Xenopus egg extract. *J. Biol. Chem.* 286:587–593. https://doi.org/10.1074/jbc.M110.181578

Wordeman, L., E.R. Steuer, M.P. Sheetz, and T. Mitchison. 1991. Chemical subdomains within the kinetochore domain of isolated CHO mitotic chromosomes. *J. Cell Biol.* 114:285–294. https://doi.org/10.1083/jcb.114.2.285

Yan, X., F. Li, Y. Liang, Y. Shen, X. Zhao, Q. Huang, and X. Zhu. 2003. Human Nudel and NudE as regulators of cytoplasmic dynein in poleward protein transport along the mitotic spindle. *Mol. Cell. Biol.* 23:1239–1250. https://doi.org/10.1128/MCB.23.4.1239-1250.2003

Zyłkiewicz, E., M. Kijańska, W.C. Choi, U. Derewenda, Z.S. Derewenda, and P.T. Stukenberg. 2011. The N-terminal coiled-coil of Ndel1 is a regulated scaffold that recruits LIS1 to dynein. *J. Cell Biol.* 192:433–445. https://doi.org/10.1083/jcb.201011142